Journal of Materials Chemistry A

Accepted Manuscript

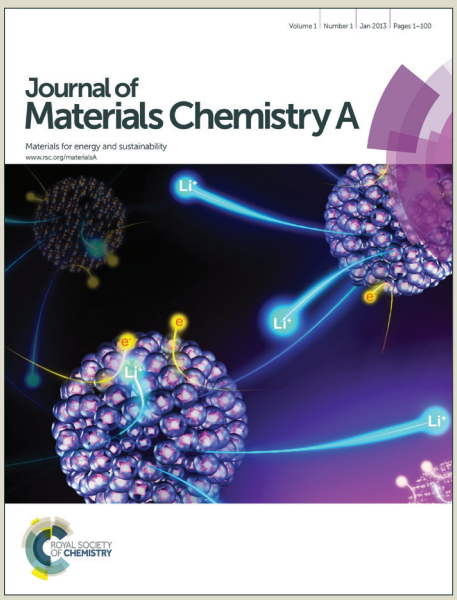

This is an *Accepted Manuscript*, which has been through the Royal Society of Chemistry peer review process and has been accepted for publication.

Accepted Manuscripts are published online shortly after acceptance, before technical editing, formatting and proof reading. Using this free service, authors can make their results available to the community, in citable form, before we publish the edited article. We will replace this *Accepted Manuscript* with the edited and formatted *Advance Article* as soon as it is available.

You can find more information about *Accepted Manuscripts* in the Information for Authors.

Please note that technical editing may introduce minor changes to the text and/or graphics, which may alter content. The journal's standard Terms & Conditions and the Ethical guidelines still apply. In no event shall the Royal Society of Chemistry be held responsible for any errors or omissions in this *Accepted Manuscript* or any consequences arising from the use of any information it contains.

ROYAL SOCIETY OF CHEMISTRY

www.rsc.org/materialsA

Journal Name

RSCPublishing

ARTICLE

High-water-content Graphene oxide/Polyvinyl alcohol Hydrogel with Excellent Mechanical Properties

Cite this: DOI: 10.1039/x0xx00000x

Yifu Huang,[a,b] Mingqiu Zhang[b] and Wenhong Ruan*[b]

Received 00th January 2012,
Accepted 00th January 2012

DOI: 10.1039/x0xx00000x

www.rsc.org/

In this study, high-water-content boron-cross-linked graphene oxide/polyvinyl alcohol (B-GO/PVA) hydrogels were prepared by freeze/thaw method and being immersed into boric acid solution for boron cross-linking. High-water-content B-GO/PVA hydrogels with the water/polymer mass ratio ranging from 19:1 to 49:1 (water content 95-98%) could be obtained. It is found that the low addition of GO can lead to significant reinforcement on the tensile strength of B-GO/PVA hydrogels with the increase in elongation. Compared to B-PVA hydrogel, 144% increase of fracture tensile strength is achieved when content of GO is 0.1 wt% (~0.609MPa, water content ~95%). Meanwhile, compression and shear strength (0.1MPa and 0.201MPa, water content ~95%) of such hydrogels are increased by 26% and 35%, respectively. A know-how of acquiring high-water-content PVA hydrogels and the reinforcing mechanism of B-GO/PVA hydrogels are suggested. It is believed that such new high-water-content hydrogels are promising in the applications of biomedical engineering and polymer electrolytes.

1. Introduction

High-water-content hydrogels can absorb and retain a significant amount of water. [1] They can be treated as aqueous materials especially when water content reaches over 95%.[2] Because of this, most of them are biocompatible, nontoxic and environmentally friendly. The creature body parts are comparative to such hydrogels for they usually contain 70~90% water. The highest water content, such as in jellyfish, can reach about 98%. Because the low content of organic or inorganic components of hydrogels benefits for the inner formation of richly porous 3D network, which in turns improves the diffusion efficiency such as in the drug and cell deliveries.[3] Besides, ion-transport behavior in the polymer hydrogel electrolyte is more similar to that of the liquid electrolyte when solvent content is ultra-high. Therefore, except for the hydrogels used in biomedical engineering,[4,5] the application range of high-water-content hydrogel can be expanded to buffer material for sports shoes, fire extinguishant, polymer hydrogel electrolyte and superabsorbent hydrogels in soilless culture etc.[2-3,6-7]

However, the problem is, most polymer-based high-water-content hydrogels have poor mechanical properties for bearing stress loading.[2,8-14] For example, some reported PAMMS or PAA based high-water-content hydrogels are too brittle to keep shape.[11] This limits the practical application of such materials. Polyvinyl alcohol (PVA) hydrogel has been well demonstrated to be biocompatible, nontoxic and balanced in mechanical properties. In recent years, it has been drawn attention to many application fields (polymer hydrogel electrolyte,[6,15] self-healing material,[16] etc.) apart from biomaterials.[17-19] The freeze/thaw method of freezing and thawing PVA aqueous solution repeatedly has attracted much attention in forming physical cross-linking hydrogel network and increasing water content of hydrogels. It is reported that the network contains three components ("free water", crystalline PVA aggregates and swollen amorphous PVA) that exist in freezing/thawing PVA hydrogels. [20] The crystalline domains act as knots of networks, swollen amorphous PVA forms porous walls and most of the water occupies the pores. It is difficult to prepare highly stable PVA hydrogel with higher water content due to the limit of such method. So far, the literatures are still blank in investigating PVA hydrogel with water percentage over 90%.[21]

To improve the water uptake of PVA hydrogels, some strategies are executed to create larger pores or more pores in the hydrogels to accommodate more water. Boric acid has been found to reduce the crystal size of PVA,[22] thus the bounding effect of crystal on molecular chains of PVA would be decreased. The released chains after reducing of crystal size may benefit for formation of larger or more pores.

On the other hand, a few reports on GO/PVA hydrogels demonstrated that GO is an excellent reinforcing nanoparticle due to its good dispersion in the PVA matrix and strong hydrogen bonding in the GO-PVA interface.[23,24] The external force can be effectively transferred to GO to promote the loading bearing of hydrogels. Interfacial interaction between GO and PVA is crucial for reinforcing effects. Physical and chemical cross-linking could enhance the interfacial interaction in GO/PVA system.[25-30]

In this study, an approach of freezing/thawing PVA aqueous solution to prepare PVA hydrogels and being followed by immersing them into boric acid solution was proposed. It is hoped that the stable PVA hydrogels with water uptake exceeding 95% could be obtained by combining physical cross-linking with boron covalently cross-linking. In order to improve the performance of cross-linked PVA hydrogel, GO sheets were

Journal of Materials Chemistry A Accepted Manuscript

incorporated into the matrix. Structure, morphology and mechanical properties of B-GO/PVA hydrogels were investigated. The reinforcing mechanism of B-GO/PVA hydrogels was suggested. The new high-water-content hydrogels with excellent mechanical properties could be anticipated.

2. Experimental section

2.1. Preparation of graphite oxide

A modified Hummer treatment of graphite flake (XF026, fixed carbon≥99.90%, 100 mesh, XF Nano, Inc., China) was used to prepare graphite oxide.[31] Firstly, 23 mL sulphuric acid (H_2SO_4, 98%) and 0.5 g sodium nitrate ($NaNO_3$, AR) were mixed together in a 250 mL beaker under ice-bath to keep the temperature below 5°C for 15 min. Then 1g graphite flake was mixed and stirred evenly. After that, 3g potassium permanganate ($KMnO_4$, AR) was slowly added into the suspension. The ice-bath was then removed and the temperature of the suspension was brought to 35°C. The reaction was maintained for at least 2 h. Then 46 mL of distilled water was slowly stirred into the mixture. The temperature was increased to 98°C and maintained for about 15 min. The suspension was then further diluted into 140 mL distilled water and treated with 2.5 mL hydrogen peroxide (H_2O_2, 30%). Filtering of the suspension was followed and a yellow-brown filter cake was got. The filter cake was washed with diluted hydrochloric acid (HCl: H_2O=1:10) to remove sulphate ions thoroughly. Finally the prepared graphite oxide was dried under vacuum at 40°C for 24 h.

To prepare graphene oxide (GO) solution, a certain amount of graphite oxide powder was dispersed in alkaline aqueous solution (V(distilled water)/V(25% ammonia solution)=100:1) with the aid of ultrasonic agitation for 20 min.

2.2. Preparation of B-GO/PVA hydrogels

To prepare hydrogels with different water content, two concentrations of PVA solutions (0.05 g/mL and 0.1 g/mL) are chosen. For 0.1 g/mL PVA solution, 25g PVA powder (alcoholysis degree>99%, average molecular weight 88,000, Aladdin reagent) was dissolved in 225mL distilled water at 95°C and mixed with 0.5mL 25% ammonia water to achieve pH~7. 10 mL of this solution was dropped and stirred into 10mL GO aqueous solution in which GO concentration ranges from 0 to 4 mg/mL. The mixture was shaken and rotated for 24h to keep it well-dispersed (pH~9.5). After that, the mixture was dumped into a 90 mm polystyrene plastic petri dish or sucked off using a 5mL plastic syringe, and if necessary, a small amount of alcohol was dropped to remove air-bubbles. The as-prepared GO/PVA hydrogels were obtained by subjecting the solution to five repeated freeze/thaw cycles, consisting of a freezing step (for 8 h at -20 °C) followed by a thawing step (for 2h at ambient temperature). To prepare chemically cross-linking B-GO/PVA hydrogels, the planar or columnar hydrogel samples were immersed in 100 mL boric acid solution (1mg/mL, pH~11) for over 48h. The corresponding dried gels were prepared by heating the hydrogels at 60 °C and further vacuum drying to remove water. The GO content of the hydrogels was expressed as weight percentage% of GO in the total weight of the samples. Additionally, the GO content in PVA phase of B-GO/PVA hydrogels was estimated with ~95wt % water, as shown in **Table 1**.

Table 1. GO content in hydrogels and in PVA phase (water content ~95 %)

GO content in hydrogels (water content ~95%) / wt %	0	0.005	0.01	0.025	0.05	0.1	0.2
GO content in PVA phase / wt %	0	0.1	0.2	0.5	1	2	4

2.3. Characterization

Morphology. Atomic force microscopy (AFM, SPM 9500J3, Japan Corporation Shimadzu) and transmission electron microscope (TEM, FEI Tecnai G2 Spirit) were used to characterize the morphology of samples.

Infrared absorption spectroscopy. Infrared absorption spectroscopy of B-GO/PVA dried gels was characterized with a Fourier infrared spectrometer (FTIR, Tensor 27, Bruker) in attenuation total reflection (ATR) mode.

Glass transition point. Glass transition temperature of dried gels was determined by a dynamic mechanical analyzer (DMA25, 01dB, Metravib instrument) equipped with tensile clamps. The testing conditions are as follows: size of samples (40 mm×10 mm×0.1 mm), dynamic displacement (1.0×10^{-5}m), frequency (1Hz), statD/dynD ratio=1.1:1, temperature range (30 °C to120 °C, ramp speed 5 °C/min).

Tensile testing. Microcomputer control electronic universal testing machine (CMT-6103, SANS Co. China) equipped with a force sensor (10N/50N) was used to measure tensile mechanical properties of hydrogels, with a gauge length of 20 mm and a drawing rate of 100 μm/s. The samples were cut to the size (~50 mm×5 mm×0.40 mm) and the mechanical test was repeated for at least 5 times to ensure the reproductivity.

Compression. Compression measurements of B-GO/PVA hydrogels were carried out by a dynamic thermal mechanical analyzer equipped with compression clamps. Alkaline hydrogels were cut to specimens (~10 mm in diameter and 3~4 mm in length). Before being tested, each sample was preloaded at 0.1 N. Stress-strain measurements were taken at a compression rate of 0.5 N min^{-1}.

Dynamic rheological properties. Rheological properties of the hydrogels were measured at the ambient temperature by an ARES-RFS controlled strain rheometer (TA Instruments), with a 25-mm-diameter para-plate attached to a transducer. The gap at the apex of the para-plate was set to be 2~3 mm.

Rebound elastic properties. Rebound elastic properties of the hydrogels in response to applied compression forces, the following programmed procedures were used (applied compression force, expressed in terms of strain; application time/rebound time in parentheses): 0%→4.8%(30 s/30 s), 0%→19.2%(30 s/30 s), 0%→38.5%(30 s/45s). Each procedure is cycled for ten times consequently.

Crystallization. X-Ray diffraction patterns of samples were obtained by Wide Angle X-ray diffractometer (WAXD, D/MAX 2200 VPC, RIGAKU) with Cu Kα radiation (30kV, 30mA). The scanning range of Bragg 2θ angle ranged from 5º to 55º under a scanning rate of 5°C/min. The size (l_c) of crystalline can be calculated using Scherrer equation:

$$l_c = \frac{0.89\lambda}{(\Delta 2\theta)\cos\theta_m}, \qquad (1)$$

Δ2θ is the half width of crystallization peak, expressed in radian; θ_m is the half peak position angle; λ is the wavelength of the X-ray.

Journal of Materials Chemistry A Accepted Manuscript

This journal is © The Royal Society of Chemistry 2012

Deswelling kinetics. The kinetics of deswelling of hydrogels were measured gravimetrically at 35°C after blotting the excess surface water with moistened filter paper. Before the measurement of deswelling kinetics, hydrogel samples reached equilibrium at room temperature, and then the hydrogel was quickly transferred into distilled water at 35°C. The weight changes of hydrogel were recorded during the course of deswelling at regular time intervals. Water retention (WR) is defined as $100\times(W_t-W_d)/W_s$, where W_t is the weight of hydrogel at regular time intervals, W_d is the weight of dried hydrogel, W_s is the weight of initial hydrogel.

Raman spectra. Raman scattering signals were detected by using Raman spectroscopy (Raman, Renishaw inVia). The excitation wavelength was 785nm with scanning range 400-3200cm^{-1}. Since there was a strong fluorescence background interference for B-GO/PVA hydrogel, before the measurement, the B-GO/PVA hydrogels were pre-treated by being immersed into hydrazine hydrate solution (2wt %) for fluorescence quenching[32] assuming the stable dispersion of GO sheets. The influence of deformation on the Raman spectra of samples was investigated.

3. Results and discussion

3.1. Structure characterization of B-GO/PVA hydrogels

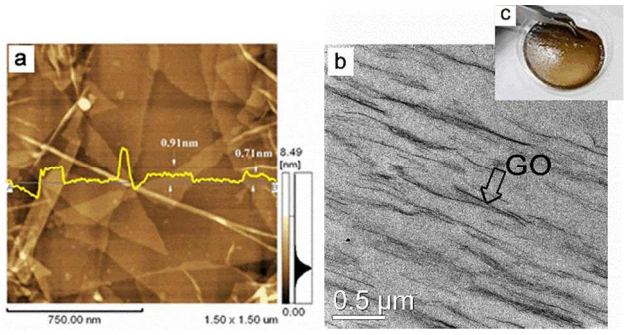

Fig. 1. (a) An AFM image in tapping mode of as-prepared GO sheets deposited on mica substrate; (b) a TEM image of dried 0.1wt %B-GO/PVA hydrogel; (c) 0.1wt %B-GO/PVA hydrogel with ~95 % water.

The AFM image of as-prepared GO sheets deposited on the mica substrate is seen in **Fig. 1**a, which indicates that the exfoliated GO sheets have an average thickness of ~1.0 nm. As shown in the TEM image of Fig. 1b, GO can be well-dispersed within PVA matrix due to similar polarity of these two components. The photo of 0.1wt % B-GO/PVA hydrogel with ~95 % water in a plastic petri dish is also shown in Fig. 1c.

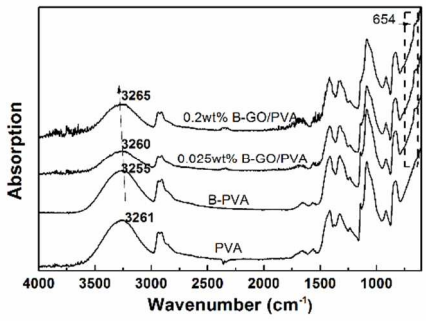

Fig. 2. Attenuation total reflectance Fourier infrared spectra (ATR-FTIR) of dried PVA, B-PVA, 0.025wt%B-GO/PVA and 0.2wt%B-GO/PVA hydrogels.

To demonstrate the boronic structure has been introduced into PVA molecular chains, the ATR-FTIR of PVA, B-PVA and B-GO/PVA films was conducted (**Fig. 2)**. Compared with typical ATR-FTIR spectra of PVA, the emerging peak at 654cm^{-1} in B-PVA and B-GO/PVA spectra is attributed to O-B-O bending.[33] While the shift of -OH stretching vibration from 3261 cm^{-1} of PVA to 3255cm^{-1} of B-PVA confirms a reduction in the number of –OH in PVA chains after the treatment with boric acid solution. This means that the boronic structure has been introduced into the PVA molecular chains. On the contrary, the -OH stretching vibration shifts from 3255 cm^{-1}of B-PVA to 3260cm^{-1} when 0.025wt % GO is incorporated, then to 3265cm^{-1} with 0.2wt % GO, indicating that the interaction between GO sheets and B-PVA is enhanced with the increase of GO content.

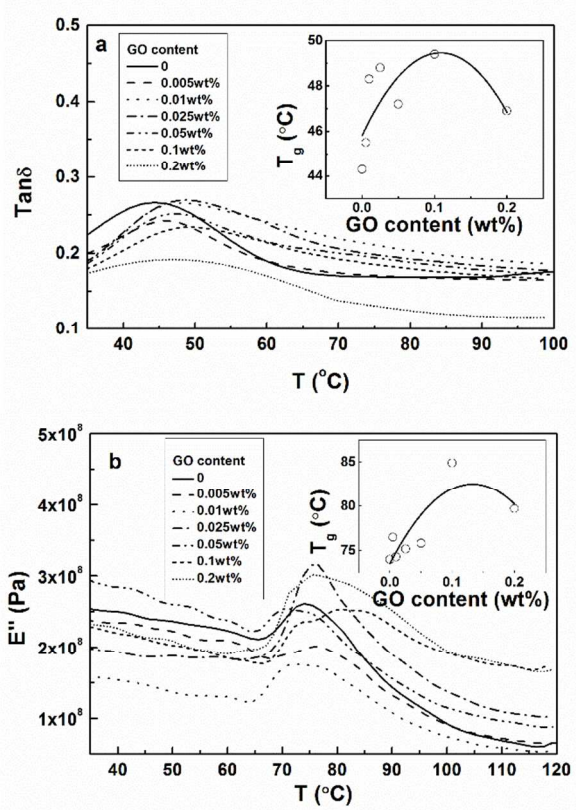

Fig. 3. DMA spectra of (a) loss tangent (tanδ) of GO/PVA and PVA samples without boron cross-linking; (b) loss modulus (E") of B-GO/PVA and B-PVA with boron cross-linking. The insets show the glass transition temperature (T_g) obtained from the peak positions of tan δ of non-boron cross-linked samples and those of E" of boron cross-linked ones.

In order to learn more about the interaction between GO sheets and PVA chains, DMA tests on the samples were carried out. The non-boron cross-linked samples have significantly different DMA behaviors from those of boron cross-linked ones (See **Fig. 3** and supplementary **Fig. 1S**). The temperature peaks appear in the tanδ curves of GO/PVA and PVA, while those appear in the E" curves of B-GO/PVA and B-PVA. Glass

Journal of Materials Chemistry A Accepted Manuscript

transition temperature (T_g) of the samples can be obtained from the peak positions of tanδ/E" curves (See the insets in Fig.3).[34] We can see that, T_g of non-cross-linked PVA is 44.3°C.The increase of GO content of the GO/PVA can bring out the increase of T_g. For 0.1wt % GO, T_g is 49.4°C. The decrease of T_g of 0.2wt %GO/PVA might be attributed to the agglomeration of the nanofillers (See supplementary **Fig. 2S**).[35] For the boron cross-linking systems, T_g of B-PVA is increased up to 74.0°C, and T_g of 0.1wt % B-GO/PVA shows 10°C increase further, almost double the increase from T_g of 0.1wt % GO/PVA to that of PVA. T_g is often related with activation energy for cooperative movement of polymer segments. So the increase of T_g would imply the enhanced interaction between filler and polymer matrix. When GO is added into PVA, T_g is increased because of hydrogen bonding interaction between PVA and GO. The restriction of covalent cross-links can slow down the PVA molecular motion effectively, so T_g of B-PVA is increased dramatically compared to that of PVA. It is worth noting that T_g of B-GO/PVA is increased further when GO reaches a certain content (0.1wt %). This indicates that motion of PVA molecular segments may be greatly restricted by the forming networks of boron cross-links and adjacent GO sheets. From the analysis of ATR-FTIR and DMA results, we can deduce that boron acid can form covalent bonds with PVA chains and being inserted into the GO sheets simultaneously because of rich hydroxyl groups on the surface of GO.

3.2. Mechanical properties of B-GO/PVA hydrogels

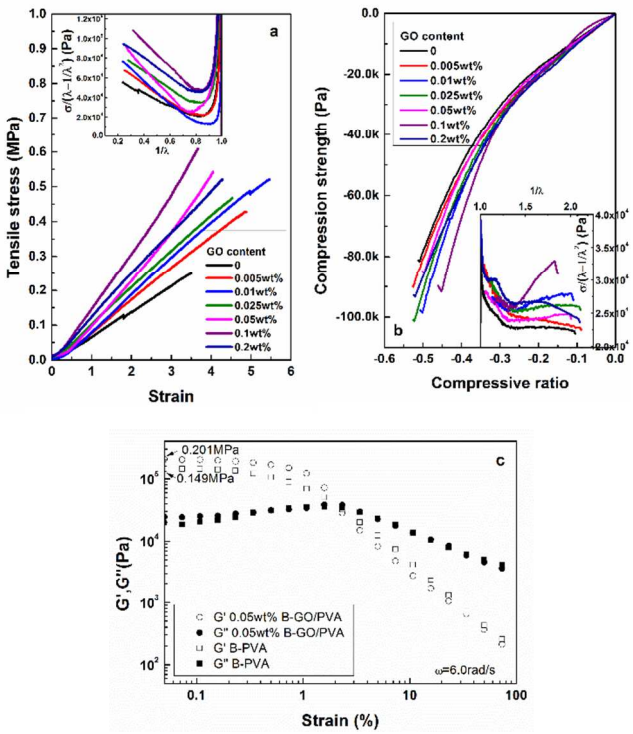

Fig. 4. Curves of mechanical properties of B-GO/PVA hydrogels (water content ~95%): (a) tensile test; (b) compression; (c) dynamic shear

Table 1. Properties of B-PVA and B-GO/PVA hydrogels

GO content /wt%		0	0.005	0.01	0.025	0.05	0.1	0.2
		Water uptake/%						
B-GO/PVA hydrogels		94.3	94.8	94.3	94.4	94.7	94.7	94.5
Fracture strength/MPa	Tensile	0.250	0.428	0.508	0.455	0.543	0.609	0.520
	Compression	-0.081	-0.087	-0.098	-0.102	-0.085	-0.092	-0.093
Elongation rate/%		350	488	547	453	405	367	428
		1/λ>1.5 (compression)						
Parameters of Mooney-Rivlin equation	$2C_1$/Pa	211	5136	8032	7854	10140	18260	25461
	$2C_2$/Pa	22492	16662	13103	9680	9757	4254	744
		1/λ<0.6(tensile)						
Parameters of Mooney-Rivlin equation	$2C_1$/Pa	7.3×10^4	9.2×10^4	1.1×10^5	1.0×10^5	1.3×10^5	1.5×10^5	1.2×10^5
	$2C_2$/Pa	-7.1×10^4	-9.5×10^4	-1.2×10^5	-8.8×10^4	-1.4×10^5	-1.3×10^5	-9.3×10^4

Fig.4a-b exhibits non-linear mechanical properties of tensile and compression behaviors of B-GO/PVA hydrogels with various GO contents (water content ~95%). The relevant properties are summarized in **Table 1**.The addition of GO leads to the reinforcement on fracture tensile strength and compression strength. 144% increase in fracture tensile strength (~0.6MPa) is gained when content of GO is 0.1 wt%. The decrease of tensile strength of 0.2 wt % B-GO/PVA is ascribed to aggregates of GO at high content.[24] The elongation of hydrogels are not sacrificed with the incorporation of GO as illustrated in Fig.4a. Compression strength is increased by 26% when GO content is 0.025wt% (See Fig.4b and Table 1).

To study the non-linear behaviors of the mechanical properties, the Mooney-Rivlin equation is used to describe the stress-strain relationship of the hydrogels,[36-37] which can be written as:

$$\sigma = \left(2C_1 + 2\frac{C_2}{\lambda}\right)\left(\lambda - \frac{1}{\lambda^2}\right), \qquad (2)$$

σ is the conditional stress, λ is the drawing ratio. The parameter $2C_1$ and $2C_2$ have been associated with the "chemical" and "physical" (intermolecular) components of transverse bonds in the polymeric basis of a binder.[35] If we set $\sigma_{red} = \sigma/(\lambda - 1/\lambda^2)$, then the linear form $\sigma_{red} = 2C_1 + 2C_2/\lambda$ is obtained (See the insets of Fig.4a-b). The parameters $2C_1$ and $2C_2$ of Mooney-Rivlin equation obtained by fitting the curves of 1/λ>1.5 (compression) or 1/λ<0.6 (tensile) are also summarized in Table 1, respectively. The quantity of $2C_2$ is related to the viscous (relaxation) component of the viscoelastic modulus.

Journal of Materials Chemistry A Accepted Manuscript

This journal is © The Royal Society of Chemistry 2012

The quantity of $2C_1$, which is related with the elastic component of the viscoelastic modulus, can be viewed as modulus of hydrogels.[38,39] The $2C_1$ of tensile and compression behaviors of B-GO/PVA hydrogels increases with GO content. The increase of $2C_1$ of compression is over 100 times when content of GO is 0.1 wt %. It means that GO has a significant effect on improvement of compression modulus of B-PVA.

The dynamic rheological properties of B-GO/PVA hydrogels are also investigated. The storage modulus (G´), which characterizes the elastic (reversible) storage of energy, and the loss modulus (G"), which characterizes the dissipation of energy, can be measured by strain amplitude sweeps of the samples (Fig.4c). The typical elastic responses of hydrogels can be seen. The G´ and G" of samples decrease rapidly above the critical strain region (γ>1.0 %), indicating a collapse of the gel state to a quasiliquid state. The incorporation of GO can benefit for improving shear strength as the G´ and G" of B-GO/PVA hydrogels are higher than those of B-PVA ones before the critical strain region. 35% increase in G´ (~0.201MPa) is achieved when content of GO is 0.1wt %. In addition, from the frequency sweep profiles of samples (See supplementary **Fig. 3S**), we can see that the G´ increases a little with frequency and becomes independent of frequency at higher frequencies, and the G" decreases at higher frequencies. The behavior of the hydrogels performs the characteristics of an elastic solid during the frequency sweep.

It is obvious that mechanical properties of PVA hydrogels decrease remarkably due to the increase of water content when the mass ratio of water/polymer raised from ~19:1 (water content ~95%) to ~49:1 (water content ~98%) (See supplementary **Fig.4S**). However, the fracture tensile strength of B-GO/PVA hydrogels (water content ~98%, GO content ~0.05wt %) is still ~0.11MPa, with 175% increase compared to B-PVA hydrogels (water content ~98%). Looking into the studies on GO/PVA systems, 132% increase in tensile strength of GO/PVA hydrogels with ~80% water uptake[24] and only 76% increase in tensile strength of GO/PVA film with ~4% water content, [25] were reported. The reinforcing effect of GO on the studied high-water-content PVA hydrogels is significant.

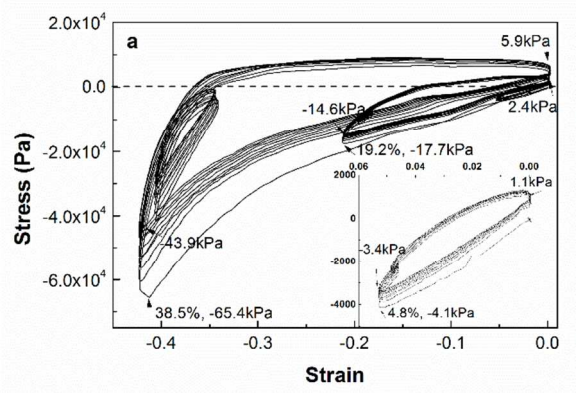

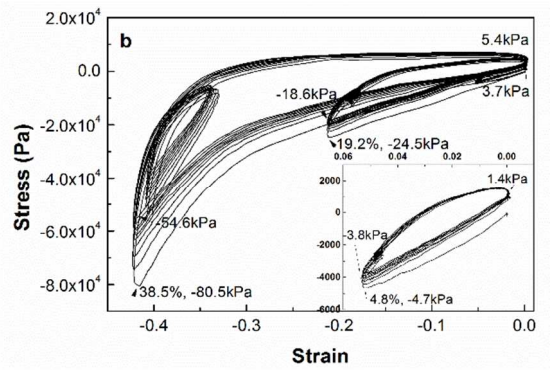

Fig. 5. Rebound elastic properties of hydrogels (water content ~95%, frequency 1Hz under ambient temperature): (a) B-PVA; (b) 0.1wt %B-GO/PVA

The rebound elasticity of B-PVA and B-GO/PVA hydrogels under different compression ratios is evaluated. As shown in **Fig.5**, the stress decays a little as the number of cycles increases owing to dehydration of hydrogels under the applied pressure. For B-PVA hydrogels, stress at maximum strain (~38.5%) decays from -65.4kPa to -43.9kPa after 10 cycles, while for B-GO/PVA ones, the stress decays from -80.5kPa to -54.6kPa. The smaller attenuation exhibits along with the smaller strain (See the insets in Fig.5). For B-PVA hydrogels, stress at 4.8% strain decays from -4.1kPa to -3.4Pa after 10 cycles, and the stress decays from -4.7kPa to -3.8Pa for B-GO/PVA ones. The studied hydrogels exhibit very rapid and stable rebound elastic properties, while the GO has little effect on improving the stability of hydrogels.

3.3. Reinforcing mechanism of B-GO/PVA hydrogels

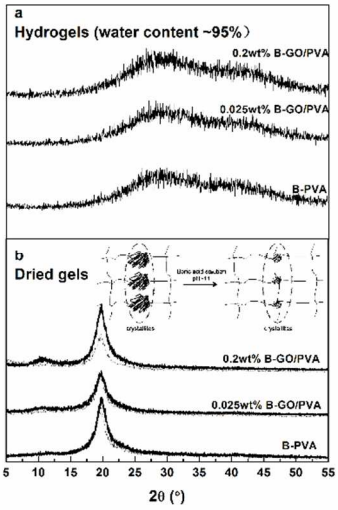

Fig. 6. Wide angle X-Ray diffraction (WAXD) patterns of (a) B-GO/PVA and B-PVA hydrogels (water content ~95%); (b) corresponding dried gels. Dashed curves in (b) represent the cases of non-boron cross-linking.

To explore the effect of boron cross-linking treatment, WAXD patterns of cross-linked and non-cross-linked hydrogels as well

Journal of Materials Chemistry A Accepted Manuscript

as corresponding dried gels are presented in **Fig. 6**. Only two halos from X-Ray diffraction signals of water lying in ~28º and ~41º are observed for all the hydrogels with ~95% water content, without any signal of PVA crystals. This is probably ascribed to the overlap of strong water signals and weak PVA crystal signals at rhe low content of polymer (~5wt %). Therefore, the effect of boron cross-linking on the crystalline is estimated from the dried state of hydrogels instead (Fig.6b). The characteristic peak of PVA crystal appears at ~20º in WAXD pattern. The half peak width of the peak is broadened after covalently cross-linking PVA hydrogel by boric acid. But GO incorporation has no evident influence on half peak width. The calculated size of crystalline (l_c) in average decreases from ~49nm to ~35nm after PVA hydrogel was covalently cross-linked. This implies that the PVA crystalline is refined and more polymer chains bounded in the crystalline are set free (See the inset of Fig. 6b) when covalently cross-linking is executed. Because of this, hydrogel network can be more expanded and water absorption of hydrogel can be further increased.

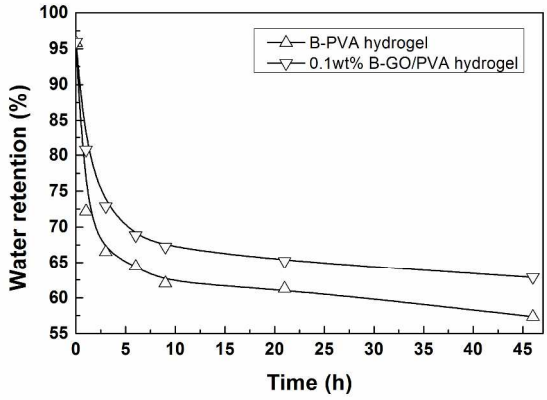

Fig. 7. Water retention of B-PVA and 0.1wt%B-GO/PVA hydrogels (water content ~95%) in distilled water at 35 ºC

To investigate the deswelling kinetics of hydrogels. The B-PVA and 0.1wt %B-GO/PVA hydrogels (water content ~95% at room temperature) are immersed in 35 ºC water environment and water retention is calculated. According to the results in **Fig.7**, we can see that equilibrated water content of hydrogels can be balanced after over 10h. 43% water loses after 46h for B-PVA hydrogels, but 38% water loses for B-GO/PVA hydrogels under the same condition when only 0.1wt %GO is added. This phenomenon shows the restriction of GO sheets on the shrinkage of B-PVA network because of strong interaction between GO and B-PVA systems.

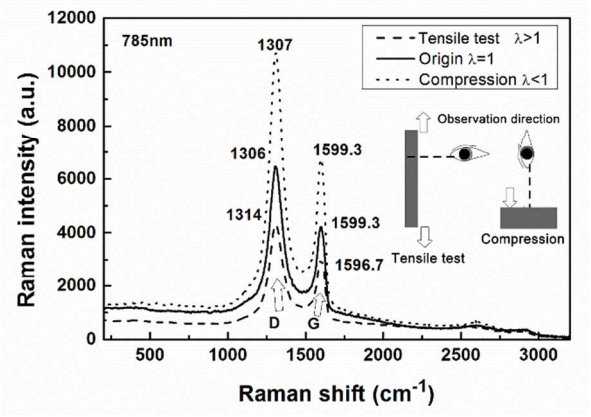

Fig. 8. Raman spectra of 0.1wt % B-GO/PVA hydrogels during the tensile test (λ>1) and compression (λ<1). The inset shows the positions where the Raman scattering signal is detected.

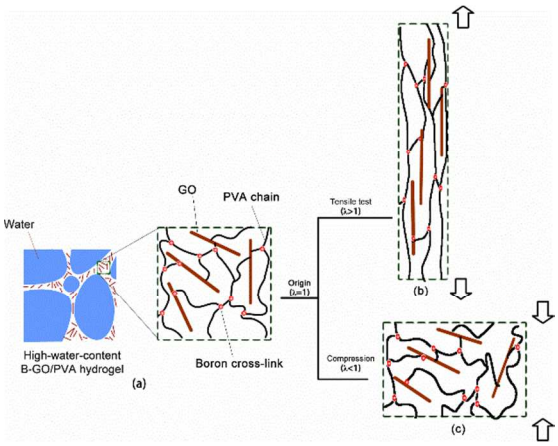

Fig. 9. Schematic drawing of tensile test and compression of B-GO/PVA hydrogel network

To explore the influence of deformation under the tensile test and compression on the arrangement of GO in the hydrogels, Raman spectra is investigated (**Fig. 8)**. The Raman spectra technology is an effective method to observe the structure of the carbon allotrope from the fingerprint, including the D peak (~1350 cm^{-1}, or disorder peak/defect peak) and the G peak (~1580cm^{-1}). The G peak position (w_G) correlates with thickness of graphene. As layers of graphene increases, w_G shifts to lower wavelength.[40] In Fig.8 we can see that G peak of B-GO/PVA hydrogel has no shift with higher Roman intensity under compression, while drawing the hydrogel causes the G peak to shift to lower wavenumber with lower intensity. It means that GO sheets within B-GO/PVA hydrogels aggregate in the direction perpendicular to tensile axial, reflecting that GO sheets are being aligned along tensile direction in fact, while neither aggregation nor dispersion of GO sheets is found under compression. The reason to account for the difference of GO arrangement is that hydrogels could experience large deformation during the tensile process. As a result, GO sheets could align along the tensile direction due to the strong

Journal of Materials Chemistry A Accepted Manuscript

This journal is © The Royal Society of Chemistry 2012

interaction between GO and B-PVA systems. Additionally, the rigid GO sheets are not only able to orient along the direction of drawing, but also to prevent effectively crack propagation by suppressing the stress concentration during the tensile test.[41] So the hydrogels with small amount GO (0-0.01wt %) added show better elongation performance. However, as the GO content (0.01-0.1wt %) increases further, the confined effect of GO on the movement of PVA due to the extensive hydrogen bonding is becoming more and more serious, so the elongation of the hydrogels are decreased. For 0.2wt % GO/PVA hydrogel, the increased elongation probably ascribes to graphene restacking that facilitated slip [42] when the aggregation of GO sheets happens.

Based on the above analysis, the schematic drawing to illustrate the mechanism of high-water-content B-GO/PVA with excellent mechanical properties are given in **Fig. 9**. Boron cross-links are introduced into PVA chains and inserted into GO sheets. A more expanded network is formed owing to the decrease in the crystal size of PVA after boron cross-linking. Stable high-water-content hydrogels can be obtained (Fig.9a). The strong interaction between GO and B-PVA benefits for stress transfer, so the deformability of hydrogels is improved as the elongation rate increases. The reinforcing effect of GO on hydrogels can come into play with the alignment of GO sheets during the tensile process (Fig.9b). On the other hand, the rearrangement of GO sheets in hydrogels is insufficient during the compression (Fig.9c). Therefore, the improvement on compression strength is not significant.

4. Conclusions

Stable high-water-content B-GO/PVA hydrogels with water uptake of 95%~98% are prepared by freeze/thaw and boron cross-linking methods. The TEM image shows that GO sheets can be well-dispersed within hydrogels. ATR-FTIR studies show that covalent boron cross-links are introduced into GO/PVA systems. The insertion of boron cross-links into GO sheets is revealed from DMA analysis. There is a strong interaction between GO sheets and B-PVA matrix. Mechanical testing results show that the addition of GO can lead to reinforce hydrogels. 144% increase (water content ~95%, GO content 0.1wt %) and 175% increase (water content ~98%, GO content 0.05wt %) in tensile strength achieve with higher elongation rate, respectively. Compression and shear strength of hydrogels (water content ~95%) are increased by 26% and 34.9%, respectively. In addition, GO has a significant reinforcing effect on the compression modulus of hydrogels. The increase of $2C_1$ of compression is over 100 times when content of GO is 0.1 wt%. The hydrogels have a stable and rapid rebound elasticity. WAXD shows the treatment of boron cross-linking reduces the crystalline size of PVA, which contributes to the higher water uptake of hydrogels. The addition of GO also benefits for the water retention of hydrogels. The Raman spectra is used to understand the arrangement of GO during the deformation of hydrogels under the tensile test and compression. The results show that GO sheets can be aligned during the tensile process, which puts reinforcing effects of GO into great play.

Acknowledgements

The authors are grateful for the support of the Natural Science Foundation of China (Grant: 51173207), Key projects of Guangdong Education Office (Grant: cxzd1101) and the Natural Science Foundation of Guangdong, China (Grants: 2011B090500004, 2012B091100313, 2012A090100006 and 2013C2FC0009).

Notes and references

[a] Key Laboratory for Polymeric Composite and Functional Materials of Ministry of Education, DSAPM Laboratory, School of Chemistry and Chemical Engineering, Sun Yat-sen University, Guangzhou 510275, China.
[b] Materials Science Institute, School of Chemistry and Chemical Engineering, Sun Yat-sen University, Guangzhou 510275, China. Email: cesrwh@mail.sysu.edu.cn

Electronic Supplementary Information (ESI) available: [details of any supplementary information available should be included here]. See DOI: 10.1039/b000000x/

1 S. K. Gulrez, S. Al-Assaf and G. O. Phillips, Progress in molecular and environmental bioengineering-from analysis and modeling to technology applications. In Tech, Winchester, 2011, ch.5, pp. 117-150.
2 Q. G. Wang, Justin L. Mynar, Masaru Yoshida, Eunji Lee, Myongsoo Lee, Kou Okuro, Kazushi Kinbara and Takuzo Aida, *Nat.* 2010, **463**, 339.
3 J-C. Gayet and G. Fortier, *J. controlled release*, 1996, **38**, 177.
4 K. Y. Lee, D. J. Mooney, *Chem. Rev*., 2001, **101**, 1869.
5 M. Hamidi, A. Azadi and P. Rafiei, *Adv. Drug Deliv. Rev.*, 2008, **60**, 16389.
6 C. M. Olympios, In Symposium on Soil and Soilless Media under Protected Cultivation in Mild Winter Climates, ISHS Acta Horticulturae 323, 1992, pp. 215-234.
7 Nohara, Shinji, Hajime Wada, Naoji Furukawa, Hiroshi Inoue, Masayuki Morita and Chiaki Iwakura, *Electrochim. Acta*, 2003, **48**, 749.
8 Eric A. Appel, Xian Jun Loh, Samuel T. Jones, Cecile A. Dreiss and Oren A. Scherman, *Biomater*., 2012, **33**, 4646.
9 J. Y. Sun, X. Zhao, W. R. Illeperuma, O. Chaudhuri, K. H. Oh, D. J. Mooney and Z. Suo, *Nat.*, 2012, **489**, 133.
10 Xiaomei Shi, Shimei Xu, Jiantao Lin, Shun Feng, Jide Wang. *Mater. Lett.*, 2009, **63**, 527.
11 Yang, Wei, Tao Bai, Louisa R. Carr, Andrew J. Keefe, Jiajie Xu, Hong Xue, Colleen A. Irvin, Shengfu Chen, Joseph Wang and Shaoyi Jiang, *Biomater.*, 2012, **33**, 7945.
12 Yasuda, Kazunori, Jian Ping Gong, Yoshinori Katsuyama, Atsushi Nakayama, Yoshie Tanabe, Eiji Kondo, Masaru Ueno and Yoshihito Osada. *Biomater.*, 2005, **26**, 4468.

Journal of Materials Chemistry A Accepted Manuscript

13 Kundu, Shyamal Kumar, Masaru Yoshida, and Mitsuhiro Shibayama., *J. Phys. Chem. B*, 2010, **114**, 1541.
14 Hyland Laura L., Marc B. Taraban, Yue Feng, Boualem Hammouda and Y. Bruce Yu., *Biopolym.*, 2012, **97**, 177.
15 J. L. Qiao, Takeo Hamaya, and Tatsuhiro Okada, *Chem. Mater.*, 2005. **17**, 2413.
16 H. J. Zhang, H. S Xia, and Y. Zhao, *ACS Macro Lett.,* 2012, **1**, 1233.
17 W. K. Wan, G. Campbell, Z. F. Zhang, A. J. Hui and D. R. Boughner, *J. Biomed. Mater Res.*, 2002, **63**, 854.
18 Nakayama, Atsushi, Akira Kakugo, J. P. Gong, Yoshihito Osada, Mitsuo Takai, Tomoki Erata, and Shin Kawano, *Adv. Funct. Mater.*, 2004, **14**, 1124.
19 Mirzan T. Razzak and Darmawan Darwis, *Radiat. Phys. Chem.*, 2001, **62**, 107.
20 Ricciardi, Rosa, Finizia Auriemma, Claudio De Rosa, and Françoise Lauprêtre. *Macromolecules*, 2004, **37**, 1921.
21 Mori, Yoshihiro, Hitoshi Tokura and Masanori Yoshikawa, *J. Mater. Sci.*, 1997, **32**, 491.
22 Miyazaki, Tsukasa, Yuuki Takeda, Sachiko Akane, Takahiko Itou, Akie Hoshiko, and Keiko En. *Polym.*, 2010, **51**, 5539.
23 H. W. Liu, S.H. Hu, Y. W. Chen and S. Y. Chen, *J. Mater. Chem.*, 2012, **22**, 17311.
24 L. Zhang, Z. P. Wang, X. Chen, Y. Li, J. P. Gao, W. Wang and Y. Liu, *J. Mater. Chem.*, 2011, **21**, 10399.
25 J. Liang, Y. Huang, L. Zhang, Y. Wang, Y. Ma, T. Guo and Y. Chen , *Adv, Funct. Mater.*, 2009, **19**, 2297..
26 S. Morimune, T. Nishino and T. Goto, *Polym. J.*, 2012. **44**, 1056.
27 J. C. Wang, X. B. Wang, C. H. Xu, M. Zhang, and X. P. Shang, *Polym. Int.*, 2011, **60**, 816.
28 Y. Y. Qi, Z. X. Tai, D. F. Sun, J. T. Chen, H. B. Ma, X. B. Yan, B. Liu and Q. J. Xue, *J. Appl. Polym. Sci.*, 2012, **127**, 1885.
29 H. K. F. Cheng, N. G. Sahoo, Y. P. Tan, Y. Pan, H. Bao, L. Li, Siew Hwa Chan and J. H. Zhao. *ACS Appl. Mater. Interfaces*, 2012. **4**, 2387.
30 Yuan, X.Y., Effective Reinforcement of Graphene in Poly (vinyl alcohol) Nanocomposites at Low Loading via Enhanced Interfacial Interaction, in Chemical Engineering and Material Properties, Pts 1 and 2, ed. H.M. Zhang and B. Wu, Trans Tech Publications Ltd: Stafa-Zurich, 2012, pp. 250-254.
31 W. S. Hummers, R. E. Offeman, *J. Am. Chem. Soc.*, 1958, **80**, 1339.
32 J. Kim, L. J. Cote, F. Kim and J. Huang, *J. Am. Chem. Soc.*, 2010, **132**, 260.
33 I. Uslu, H. Daştan, A. Altaş, A. Yayli, O. Atakol and M. L. Aksu, e Polym., 2007, **133**, 1.
34 Park, J. S., Park, J. W. and Ruckenstein, E. hydrogels. *Polymer*, 2001, **42**, 4271-4280.
35 Xiang, C., Cox, P. J., Kukovecz, A., Genorio, B., Hashim, D. P., Yan, Z, et.al. *ACS nano*, 2013, 7, 10380-10386.
36 N.Sanabria-DeLong, A.J. Crosby and G.N. Tew, *Biomacromolecules*, 2008. **9**, 2784.
37 T. Wang, L. Dan, C. X. Lian, S. D. Zheng, X. X. Liu and T. Zhen, *Soft Matter*, 2012, **8**, 774.
38 Ermilov, A. S. and E. M. Nurullaev, *Mech. Compos. Mater.*, 2012, **48**, 1.
39 A. V. Dobrynin and J. M. Y. Carrillo, *Macromol.*, 2010, **44**, 140.
40 H. Wang, Y. F. Wang, X. W. Cao, M. Feng, and G. X. Lan, *J. Raman Spectrosc.*, 2009, **40**, 1791.
41 Shen, J., Yan, B., Li, T., Long, Y., Li, N., and Ye, M. *Soft Matter*, 2012, 8, 1831-1836.
42 Wang, R., Sun, J., Gao, L., Xu, C. and Zhang, J. *Chem. Commun.*, 2011, 47, 8650–8652.

Journal of Materials Chemistry A Accepted Manuscript

This journal is © The Royal Society of Chemistry 2012

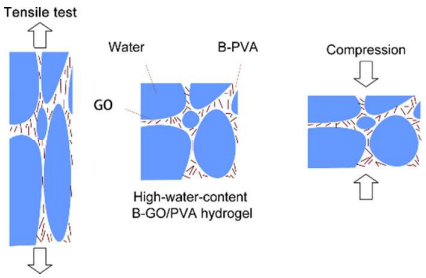

Boron-crosslinked graphene oxide/polyvinyl alcohol (B-GO/PVA) hydrogels with high-water-content and excellent mechanical properties are prepared by freeze/thaw and boron cross-linking methods.

Journal of Materials Chemistry A Accepted Manuscript